ISSN 0915-633X

NATIONAL INSTITUTE FOR FUSION SCIENCE

Possible Control Scenario of Radial Electric Field by Loss-Cone-Particle Injection into Helical Device

O. Motojima, A.A. Shishkin, S. Inagaki and K.Y. Watanabe

(Received - July 22, 1999)

NIFS-607 Aug. 1999

RESEARCH REPORT
NIFS Series

NAGOYA, JAPAN

Possible Control Scenario of Radial Electric Field by Loss-Cone-Particle Injection into Helical Device

Osamu MOTOJIMA, Alexander A. SHISHKIN*, Shigeru INAGAKI, Kiyomasa Y.WATANABE

National Institute for Fusion Science, Toki 509-5292, JAPAN

*Permanent address: National Science Center "Kharkov Institute of Physics and Technology", Kharkov-108, Ukraine

Abstract.

The possibility of controlling the radial electric field of toroidal plasmas by injecting high energy electrons along the reversible loss cone orbit of the helical magnetic traps is investigated. It is well known that the radial electric field plays an important role in the confinement improvement scenario especially in the low collisional regime under the physics picture of neoclassical theory. For this purpose, it is made clear that the most suitable particles are transit particles, which show a transition from helically trapped orbits to blocked ones It is also found that a parallel AC electric field launched from outside assists this transition and makes it possible for particles to penetrate deeply into the plasma. In addition we clarify that the viscosity of the plasma coupled with the helical field configuration provide a bifurcation of plasma states and its stable solution results in confinement improvement.

Keywords: helical system, loss cone, particle orbit, electric field, bifurcation, confinement improvement.

1 Introduction

It is commonly understood that radial electric field plays an important role in improving the confinement properties of helical type magnetic traps like the Large Helical Device (LHD) [1, 2] especially in the low collisional regime under the physics picture of the neoclassical theory [3]. As one of the possible ways to control the radial electric field of plasmas a new idea is proposed which is to inject high energy electrons or ions into the plasma core. However, it is not easy to bring charged particles freely into the core region across a strong toroidal magnetic field According to previous tokamak studies, one proposal was made to introduce an additional ripple field to modify its symmetric field in order to transport particles into the core region along ripple trapped drift orbits [4] On the contrary, in the case of LHD, it is possible to utilize the existing loss cone orbit, which has a reversible characteristic. Usually, these loss cone orbits should be minimized during field design optimization to reduce direct particle loss and to increase the confinement capability. In practice, in the case of LHD, the magnetic field has been optimized such that inside the one-third in minor radius ($r<a_p/3$, where a_p is the plasma radius) it has no loss cone orbit [5]. Therefore, again we need to choose the appropriate particles, which will possibly reach to the central core of the plasma. The candidate orbit for this scenario is the transit particles, which show transitions from helically trapped orbits to blocked ones [6-12]. In this paper we demonstrate the existence of such a reversible loss cone orbit and that it works well to supply high energy particles into the core. At the same time, we investigated the effect of an assisting AC electric field launched from the outside, which helps this transition. Here, we observed that there is a range of adjustable parameters, such as the ratio of the parallel velocity to the total velocity $V_{//}/V$ and the positions of the starting points of particles. In addition we clarify that the viscosity of the plasma coupled with the helical field configuration provides a bifurcation of plasma states and its stable solution results in the confinement improvement.

The size of the loss cones depends on the magnetic field spectrum in angular variables or, in other words, the type of the modulation of the magnetic field along the force line. The Large Helical Device (LHD) is a very flexible device and different types of magnetic configurations can be realized [13]. For our study, a special

configuration is taken, in which the major radius of the magnetic axis (R_{ax}) is shifted outside (R_{ax} = 3.9 m) compared to the standard configuration (R_{ax} = 3.75 m). It was made clear that the outer shifted configuration is favorable for the transition of the particles from the helically trapped to the blocked, and even helps them to be a passing particle in the core of plasma.

This paper is composed in the following way. In Section 2 properties of loss cone orbits of the high energy electrons are considered for the LHD configuration. Penetration
of high energy electrons is studied. The effect of the longitudinal AC electric field is investigated to enhance the appropriate transition in the core region from the trapped to the blocked and to avoid the retrapping of the particles, which would lead to the loss of injected particles. Section 3 is devoted to the viscosity analysis concerned with the configurations of LHD, which provide a bifurcation of possible plasma state and confinement improvement. The main conclusions are given in Section 4

2. Helical Field Ripple Loss Cone as a Means for the Penetration of High Energy Electrons to the Plasma Core

2.1 Main Equations for Orbit Analysis, Magnetic and Electric Field Models

2.1.1. Guiding Center Equations

For the orbit analysis the equations of the particle motion in the guiding center drift approximation are used [14]

$$\frac{d\boldsymbol{r}}{dt} = V_{//}\frac{\boldsymbol{B}}{B} + \frac{c}{B^2}[\boldsymbol{E}\times\boldsymbol{B}] + \frac{M_j c\left(2V_{//}^2 + V_\perp^2\right)}{2e_j B^3}[\boldsymbol{B}\times\nabla B]$$

,

$$\frac{dW}{dt} = eE\frac{d\boldsymbol{r}}{dt} + \frac{M_j V_\perp^2}{2B}\frac{\partial B}{\partial t}, \qquad (1)$$

$$\frac{d\mu}{dt} = 0,$$

where W is the kinetic energy of the particle, $V_\perp$ and $V_{//}$ are the perpendicular and parallel velocities of the particle, M_j and e_j are the mass and charge of the particle, $\boldsymbol{B}$ is the magnetic field, $\boldsymbol{E}$ is the electric field, μ is the magnetic moment of the particle ($\mu = M_j V_\perp{}^2 / 2B$), and r is the vector-radius of the particle guiding center.

2.1.2. Magnetic Field Model

The magnetic field is modeled with the scalar potential ($\boldsymbol{B} = \nabla\Phi$)

$$\Phi = B_0\left[R\varphi - \frac{R}{m}\sum_n \varepsilon_{n,m}(r/a_h)^n \sin(n\vartheta - m\varphi) + \varepsilon_{1,0} r\sin\vartheta\right], \qquad (2)$$

where B_0 is the magnetic field at the circular axis, R and a_h are the major and minor radii of the helical winding, r, ϑ, φ are the coordinates connected with the circular axis of torus. Then r is the radial variable, and ϑ (φ) is the angular variables along the minor (major) circumferences of the torus, ϑ is accounted from the direction of the main normal to the circular axis of the torus. Metric coefficients are the following: h_r=1, h_ϑ=r, h_φ= R-$r\cos\vartheta$; m is the number of the magnetic field periods along the torus, l is the helical winding pole number. Index n=l, l-1, l+1; $\varepsilon_{n,m}$ are the numerical coefficients in the expression for Φ. For the results presented here l=2, m=10, B_0 =3 T, R=3.90 m, a_h=0.975 m the parameter values $\varepsilon_{n,m}$ are taken in such way that the magnetic surfaces and the magnetic field modulation coincide with the results [13]. For the case of the outer shifted configuration considered here $\varepsilon_{2,10}$= 0.76, $\varepsilon_{3,10}$= -0.032, $\varepsilon_{1,10}$= -0.056, $\varepsilon_{1,0}$= 0.07. Here the right hand system of coordinates is used and the magnetic field direction is pointed counterclockwise when viewed from the top, and hence the ∇B drift (toroidal field) is upward for ions and is downward for electrons.

2.1.3. Model of the Electric Field in Plasma

The electric field in the plasma can be described in the general case with the following scalar potential

$$\phi = \phi_0 \Psi^q \left(0.5 - \Psi^g\right)^p \exp(-k\Psi), \qquad (3)$$

where the function Ψ describes the cross-sections of the magnetic surfaces

$$\Psi = A\left[\left(\frac{r}{a_h}\right)^2 + \frac{2}{m^2}\left(\frac{R}{a_h}\right)^2 \times\sum_n n\varepsilon_{n,m}\left(\frac{r}{a_h}\right)^n \cos(n\vartheta - m\varphi)\right], \qquad (4)$$

here the summation index n=l, l-1, l+1; constant A is taken as A=1.3a_p/a_h. The parameter q, g and p in Eq. (3) control the profile of the electric field potential. The values of these parameters are given in Section 2.2.2

2.1.4. AC Electric Field Model

In the consideration here the AC electric field parallel to the magnetic force line is taken in the form

$$\tilde{E}_{\varphi} = \sum_{n,m,\Omega}\left[\tilde{E}^{c}_{n,m,\Omega}\cos(n\vartheta - m\varphi) + \tilde{E}^{s}_{n,m,\Omega}\sin(n\vartheta - m\varphi)\right]\cos(\Omega t + \delta), \quad (5)$$

where $\tilde{E}^{c}_{n,m,\Omega}$ ($\tilde{E}^{s}_{n,m,\Omega}$) is the amplitude of the AC electric filed, Ω and δ are the frequency and the phase of the field, respectively. Parameter values are given in the Section 2.3.

2.2 Penetration of High Energy Electrons to the Core of the Magnetic Confinement Volume

2.2.1.Analytical Treatment

For the purpose of studying the penetration of injected high energy electrons, it may be helpful to consider the transition curve equation and, particularly, to study the effect of the electric potential profile on the de/re-trapping of the particle.

Transition Equation

As the transformation of the particles from the helically trapped into blocked or passing ones is of interest, it is necessary to consider the transition equation which can be obtained from the longitudinal adiabatic invariant $J_{//} = \oint V_{//}\, dl$ derived for the particles trapped in the helical field ripples. The expression for the $J_{//}$ has the following form

$$J_{//} = \frac{16R}{m}\sqrt{\mu B_0}\sqrt{\tilde{\varepsilon}_{l\phi}}\left[\mathrm{E}(\mathrm{q}^2) - (1-\mathrm{q}^2)\mathrm{K}(\mathrm{q}^2)\right], \quad (6)$$

where $\mathrm{E}(\mathrm{q}^2)$ and $\mathrm{K}(\mathrm{q}^2)$ are the complete elliptic integrals of the first and second kind, q^2 is the modulus of elliptic integrals of the form [13]

$$\mathrm{q}^2 = \frac{1}{2} + \frac{1}{2\tilde{\varepsilon}_{l\phi}} \times\left(\frac{W - e\phi_0 - e\phi_1\sin\vartheta_0}{\mu B_0} - \varepsilon_t\cos\vartheta_0 - 1\right). \quad (7)$$

Here the electric field potential ϕ is taken into account in the simplified form

$$\phi = \phi_0 + \phi_1\sin\vartheta_0 + \sum_n \phi_{n,m}\sin(n\vartheta_0 - m\varphi), \quad (8)$$

where the index of summation $n=l$, l-1, l+1 The coefficients $\varepsilon_{n,m}$ and $\phi_{n,m}$ enter in Eq (7) through

$$\tilde{\varepsilon}_{l\phi} = \left[\tilde{\varepsilon}_l^{\,2} + \left(\frac{e\tilde{\phi}_l}{\mu B_0}\right)^2 + 2\frac{e\tilde{\phi}_l}{\mu B_0}\tilde{\varepsilon}_l(\mathrm{BD} - \mathrm{AC})\right]^{1/2}, \quad (9)$$

where

$$\tilde{\varepsilon}_l = \varepsilon_{l,m}\left(\mathrm{A}^2 + \mathrm{B}^2\right)^{1/2},$$
$$\tilde{\phi}_l = \phi_{l,m}\left(\mathrm{C}^2 + \mathrm{D}^2\right)^{1/2},$$

$$\mathrm{A} = \sum_n \frac{\varepsilon_{n,m}}{\varepsilon_{l,m}}\sin n\vartheta_0,$$
$$\mathrm{C} = \sum_n \frac{\phi_{n,m}}{\phi_{l,m}}\sin n\vartheta_0, \quad (10)$$
$$\mathrm{B} = \sum_n \frac{\varepsilon_{n,m}}{\varepsilon_{l,m}}\cos n\vartheta_0,$$
$$\mathrm{D} = \sum_n \frac{\phi_{n,m}}{\phi_{l,m}}\cos n\vartheta_0.$$

Here index of summation n=0, 1, 2, .., $\varepsilon_t = a/R_0$ and r_0 and ϑ_0 are the coordinates of the particle launching points. The equation q^2=1 (transition equation) determines the curve which separates the geometrical regions in r_0, ϑ_0 space of the helically trapped and blocked particles under the given values of the parameters $W/\mu B_0$, $e\phi_0/\mu B_0$, ε_l, ε_t etc.. Inside the region surrounded with this curve the particles have the well-depth parameter q^2>1, these are the passing particles. Outside the region there are the particles with a well-depth parameter q^2<1, these are helically trapped particles. Those particles which cross the curve q^2=1 (transition curve) change their state, these are the particles with the transit orbits.

Let us consider the transition equation in some specific cases.

a). In the simplest case, when only two main harmonics of the magnetic field (with $\varepsilon_{2,10}$ and ε_t) are taken into account, the transition curve is described with the equation of the circumference which in the variables $x=(r_0/a)\cos\vartheta_0$, $x=(r_0/a)\sin\vartheta_0$ takes the following form

$$(x + \Delta_t)^2 + y^2 = R_t^{\,2}, \quad (11)$$

the radius of this curve R_t and the shift of the center of the circumference Δ_t are connected with other parameters in such a way

$$R_t^2 = \frac{1}{4}\left(\frac{\varepsilon_t}{\varepsilon_{2,10}}\right)^2 + \frac{\lambda^2}{\varepsilon_{2,10}^2},$$

$$\Delta_t = \frac{1}{2}\frac{\varepsilon_t}{\varepsilon_{2,10}}. \qquad (12)$$

Parameter $\lambda^2=(V_{//0}/V_{\perp 0})^2$ is expressed through the values of the velocity components at the point where magnetic field is equal to B_0.

b). If the nearest satellite harmonics with small coefficients $\varepsilon_{1,10}$ and $\varepsilon_{3,10}$ are taken into account in the magnetic field, the determination of the transition equation, obtained by the perturbation method, takes the form

$$\frac{r_0}{a} = \left(\frac{r_0}{a}\right)_0 - \left[\varepsilon_{3,10}\left(\frac{r_0}{a}\right)_0^3 + \varepsilon_{1,10}\left(\frac{r_0}{a}\right)_0\right] \times \cos\vartheta_0 \frac{1}{2\varepsilon_{2,10}\left(\frac{r_0}{a}\right)_0 - \varepsilon_t\cos\vartheta_0}. \qquad (13)$$

where

$$\left(\frac{r_0}{a}\right)_0 = -\frac{1}{2}\frac{\varepsilon_t}{\varepsilon_{2,10}}\cos\vartheta_0 + \sqrt{\varepsilon_t^2\cos^2\vartheta_0 + 4\varepsilon_{2,10}\lambda^2}. \qquad (14)$$

The perturbation approach can be used here because the nearest satellite harmonics are much smaller than two main harmonics ($\varepsilon_{1,10}/\varepsilon_t$ = -0.18, $\varepsilon_{3,10}/\varepsilon_t$ = 0.10, $\varepsilon_{1,10}/\varepsilon_{2,10}$ = -0.073 and $\varepsilon_{3,10}/\varepsilon_{2,10}$ = 0.042). From Eq. (13) one can see that the radius of the transition curve depends on not only the value but also the sign of the satellite harmonics.

The families of the transition curves when the satellite harmonics are taken into account are shown on Fig. 1 (a). They are depicted on the background of the magnetic surfaces in two vertical cross-sections. These transition curves are obtained for the set of parameter $V_{//0}/V$ values: $V_{//0}/V$ =0.01, 0.11, 0.21 and 0.31.

c) When the electric field potential is taken into account, the transition curve is also affected. The radius of transition curve depends on the value and the sign of $e\phi_0/\mu B_0$, as shown in Fig. 1(b) (only upper parts of the transition curves are shown except in $e\phi_0/\mu B_0$=0.0 case). With respect to this figure, $V_{//0}/V$ = 0.31 and the parameters of the profile of the electric field given by Eq. (3) are employed as q=1, p=0 and k=2, respectively. The magnetic surfaces in a typical vertical cross-section are also shown.

2.2.2. Numerical Integration of Guiding Center Equations

Electric Field Profile

For our numerical examples the outer shifted magnetic configuration, in which the major radius of the magnetic axis is shifted outside compared to the standard configuration, is considered. The electron energy W =150 keV and the electric field is taken as $e\phi_0/W$=0.1, the profile of the electric field is chosen under the following parameter values: k=5, q=1, g=0 and p=1. We employ the "parabolic" profile (Fig.2) because of similar parabolic profiles of the electric field in the plasma can be expected from the neoclassical analysis. Such profile of the electric field can be unfavorable for the penetration of electrons in the core of plasma.

When electrons accumulate to the core of plasma, the electric field profile becomes deeper. Then the penetration of each additional electron becomes more difficult. This fact takes place in a tokamak [4]. And it can also take place in the helical magnetic field. However, the time evolution of the electric field profile is not taken into account here.

Motion of Electron with Transit Orbit from "Loss Cone"

The launching points of the high energy electrons are on the paths of the trajectories leading to the "loss cone orbits". Namely these are the points where the electron gun should be placed In the actual device there are vertical ports which can be used to insert the electron gun. The launching point of our calculation has the following coordinates: r_0=50.18 cm, ϑ_0=6.291 radian and φ_0=2.144 radian.

The trajectory of the electron with $V_{//0}/V$ = -0.161 follows to the "loss cone orbit". This particle is helically trapped at the beginning and then it makes transition to be blocked (de-traps). However after t=4.76×10^{-5} sec it becomes helically trapped again (re-trapping takes place). These processes are illustrated in Figs.3 and 4. The projection of the trajectory of the particle on the vertical plane (Fig.3.a) is shown with the magnetic surfaces

calculated on one meridian cross-section. The transformation of the particle from the helically trapped into a blocked one (in the r_0, ϑ_0 - space) is in conformance with the position of the transition curve obtained under $V_{//0}/V$ =0.01 The projection of the trajectory on the horizontal plane can be seen on Fig 3 b. The full 3-dimensional (3D) trajectory (Fig 4 a) is followed until retrapping occurs The moment of retrapping of the particle can be seen from the change of $V_{//0}/V$ on time (Fig. 4 b). The retrapping occurs at t =1 76×10^{-5} sec, and $V_{//0}/V \leq 0.01$

The time that the transit particle stays in the blocked state can be small to achieve the desirable effect Therefore several possibilities to extend the time of particle staying in the blocked state are considered

2.3 The Possibility to Extend the Stay of the Particle in the Plasma Core with the Use of an AC Electric Field

Retrapping of the transit particle can be postponed if an AC electric field is applied parallel to the magnetic force line. The possibility of the conversion of the trapped particle into an untrapped one in the parallel AC electric field is well known already [15, 16]. An AC electric field has been used experimentally for the reduction of the neoclassical transport caused by the helically trapped particles [17].

Here the effect of an AC electric field is investigated as a physically new application to extend the time in which the particle stays in the blocked state, i.e. to delay the time of retrapping

2.3.1.Analytical Treatment

Effect on Trapped Particles

The possible effect on the transformation of the particle from a helically trapped one into helically untrapped particle can be seen from the equation for $dV_{//}/dt$ which is follows from the system of Eqs (1). In the simplest case of one helical harmonic in the magnetic field, this equation takes the form

$$\frac{dV_{//}}{dt} = -\frac{\mu}{M_j}\frac{B_0}{R} m\varepsilon_l \left(\frac{r}{a}\right)^l \cos(l\vartheta - m\varphi) + \frac{e\tilde{E}_\varphi}{M_j}\left\{1 - \frac{V_{//}}{\omega_c}\frac{1}{a}\left[\frac{Rl}{ma}\varepsilon_l\left(\frac{r}{a}\right)^{l-1} \times \cos((l-1)\vartheta - m\varphi) + \frac{Rl}{ma}\varepsilon_l^2 l\left(\frac{r}{a}\right)^{2(l-1)}\right]\right\}. \quad (15)$$

If the AC electric field $\tilde{E}_\varphi$ in Eq (5) is applied and its period is comparable with the period of the motion of particle, one can expect the influence on the change of $V_{//}$ in time.

For the helically trapped particle the bounce period $\tau_{bh} = \oint dl / V_{//}$ can be expressed in the following form

$$\tau_{bh} = 4\sqrt{2}\frac{R}{mV_{\perp 0}^2}\frac{1}{\sqrt{\varepsilon_l (r_0/a)^l}} \mathrm{K}(q^2), \quad (16)$$

where

$$q^2 = \frac{(V_{//0}^2/V_{\perp 0}^2) - \varepsilon_l (r_0/a)\cos\vartheta_0}{2\varepsilon_l (r_0/a)^l} - \frac{1}{2}. \quad (17)$$

Here, for simplicity, one helical harmonic is taken into account

In the case where the bounce frequency ω_b (ω_b=2π/τ_{bh}) is comparable with the AC electric field frequency Ω, the contribution from $\tilde{E}_\varphi$, namely

$$\frac{eE^c_{2,10,\Omega}}{M_j}\cos(l\vartheta - m\varphi)\cos(\Omega t + \delta), \quad (18)$$

competing with

$$-\frac{\mu}{M_j}\frac{B_0}{R} m\varepsilon_l \left(\frac{r}{a}\right)^l \cos(l\vartheta - m\varphi), \quad (19)$$

can change $dV_{//}/dt$ and affect the processes of de/re-trapping of the particles.

Possibility to Reduce the Drift Velocity

It should be noticed also that in principle the parallel AC electric field can effect the drift velocity of particles which is connected with the gradient of the magnetic field It can be seen from the equations of guiding center motion if one expresses them in terms of variables $x=r\cos\vartheta$, $y=r\sin\vartheta$.

$$\frac{dx}{dt} = -V_{//}\frac{2R}{ma}\varepsilon_2 (y\cos(m\varphi) - x\sin(m\varphi)) + \frac{c}{B^2}\tilde{E}_\varphi B_0 \frac{2R}{ma}\varepsilon_2 (x\cos(m\varphi) + y\sin(m\varphi)) + \frac{V^2 + V_{//}^2}{\omega_c}\varepsilon_2 \frac{1}{a}(y\cos(m\varphi) - x\sin(m\varphi)), \quad (20)$$

$$\frac{dy}{dt} = -V_{//}\frac{2R}{ma}\varepsilon_2\left(x\cos(m\varphi)+y\sin(m\varphi)\right) - \frac{c}{B^2}\tilde{E}_\varphi B_0\frac{2R}{ma}\varepsilon_2\left(y\cos(m\varphi)-x\sin(m\varphi)\right) + \frac{V^2+V_{//}^2}{2\omega_c}\left[\varepsilon_t\frac{1}{a}+\varepsilon_2\frac{2}{a}\left(x\cos(m\varphi)+y\sin(m\varphi)\right)\right].$$

The part of the contribution from the second term on the right hand side of the equation for dy/dt which is proportional to the AC electric field $\tilde{E}_\varphi$, can been the following:

$$\frac{\tilde{E}_{2,10,\Omega}}{B_0}\varepsilon_t\frac{R}{ma}\varepsilon_2\left(\frac{r_0}{a}\right)^2\sin(\Omega t+\delta). \qquad (21)$$

During half of the period of the $\tilde{E}_\varphi$ variation, this term can decrease the drift velocity by

$$\frac{V^2+V_{//}^2}{2\omega_c}\varepsilon_t\frac{1}{a}, \qquad (22)$$

while this term increases the drift velocity during the other half period

2.3.2. Numerical Study

Here some characteristic cases are considered.

Motion of Transit Electron with AC Electric Field

If $\Omega \approx (1/2)\omega_b$, the particle remains in the blocked state, i.e. it isn't retrapped by more than twice as long (Fig.5) compared with the case described above (subsection 2.2.2). Where Ω is the cycle of the externally applied electric field and ω_b is the bounce frequency of the helically trapped particle at the point of the transition. The value of the bounce frequency is near 0.45×10^7 1/sec. To consider its effect upon the particle, two nonzero parameters $\tilde{E}_{0,0,\Omega}$ and $\tilde{E}_{2,10,\Omega}$ are taken, where $\left|\tilde{E}_\varphi\right|_{max}/\left|E_r\right|_{max}=0.5$. Here $\left|E_r\right|_{max}$ is the absolute maximum of the electric field component E_r in the plasma and $\left|\tilde{E}_\varphi\right|_{max}$ is the absolute maximum of the AC electric field $\tilde{E}_\varphi$ on the trajectory of the particle.

The 3D trajectory (Fig. 5 a) is shown after $t = 1.07\times10^{-4}$ sec. The staying time in the blocked state becomes longer, namely $t = 1.32\times10^{-4}$ sec. (Fig. 5 b). The physical explanation of this effect can be seen from the comparison of the $V_{//}/V$ as a function of the time between with and without the AC electric field (Fig. 6). The decrease of the parallel velocity at the moment of detrapping under the AC electric field is compared with the case without (Fig. 6 a). The AC electric field causes the essential delay of the process of retrapping (Fig.6 b). In the figures the AC electric field is shown in dimensionless units. These particles are helically trapped at the launching point and become blocked particles at the point of the transition ($V_{//}/V$ =- 0.161 at the launching point). The AC electric field is effective in prolonging the duration of the blocked state.

Motion of Deeply Trapped Particle without AC Electric Field

Trapped particles are important if one would like to increase the number of particle, which can penetrate to the center of the confinement volume and stay there. Under small values of the parameter $V_{//}/V$, namely $V_{//}/V$ = -0.03 at the launching point, the trajectory of the electron shown is the typical one of the deeply trapped particle belonging to the "loss cone" (Fig.7 a). The particle is helically trapped from the beginning and lost (Fig.8 a) during the time of observation $t = 4.76\times10^{-5}$ sec.

The question is how to transform the deeply trapped particles into the blocked state. The answer would mean to extend the class of the particles (to make a wide range of $V_{//}/V$) which can penetrate into the core and stay there for a necessary time. Again the AC electric field can be helpful. It is possible to transform the helically trapped particles into the blocked state for some time.

Motion of Trapped Electrons under AC Electric Field Applied at the Point where Transition Is Desirable

Now we consider the particles, which are helically trapped in the absence of the AC electric field. They do not detrap under $\tilde{E}_\varphi$=0. The pitch angle velocity of these particles is smaller than that of the transit particles. Our typical example here is the case $V_{//}/V$ = -0.03. It is possible to improve the orbit of the particles with a larger pitch angle in velocity with the AC electric field at the point where the transition takes place (transit particles). In such way the particles with smaller parallel velocity being deeply helical trapped experience the transition under finite $\tilde{E}_\varphi$ and become blocked particles (Figs.7 b, c and 8 b, c). Under the approximate condition $\Omega\approx(3/2)\omega_b$ particles

remains in the blocked state (Fig. 7 b) until the time t =3 7×10^{-5} sec. (Fig.8 b). Then they are retrapped again and it is possible to see the new turns of helically trapped particle on the plot of a 3D trajectory (Fig. 7 b). In the case of Ω=(5/2)ω_b the particle stays in the blocked state (Fig 8 c) much longer, until the time t =1 3×10^{-4} sec. (Fig. 8 c).

Sensitivity of the Losing Time in the Blocked State on the Launching Point Position

The length of time for which particle spends in the blocked state is evaluated and shown in Fig. 9. This is a result measured by changing the launching position. The time τ, which the particle spends in the blocked state, is determined as the interval between the time of retrapping and the time of detrapping. Figure 9 indicates that a difference of true launching points by 1 cm does not show a large effect. This is an important result to design an appropriate electron gun.

3. Viscosity Properties of the LHD Configuration.

3.1. Basic equations

Anomalous transport has played a more dominant role than neoclassical transport in toroidal plasmas. Some theories for turbulence predict that the anomalous transport caused by plasma fluctuations is influenced by the radial electric field through its inhomogeneity [18, 19]. Thus, it is important to investigate the mechanisms of transport by generating a radial electric field. If the loss mechanisms, which are not intrinsically ambipolar, are present, the radial electric field is decided by the condition that the total particle flux is ambipolar in steady state. If electrons are injected into the plasma, the radial electric field will build up negatively, unless the plasma reacts by changing compensating non-ambipolar fluxes equal to the injected electron flux. Each of these fluxes, such as the loss of ions [20], the diffusion flux introduced by helically trapped particles [21] and the flux due to the bulk ion viscosity [22] has a non-linear dependence on the radial electric field, and hence the drastic change of the radial electric field is expected.

There are many processes which are associated with the non-ambipolar flux and hence

$$\frac{\varepsilon_0\varepsilon_\perp}{e}\frac{\partial E_r}{\partial t} = \Gamma_e^{nc} - \Gamma_e^{beam} - \Gamma_i^{nc} - \Gamma_i^{lc} - \Gamma_i^{bv} - \Gamma_i^{cx}, \quad (23)$$

Poisson's equation can be written as [23]

where ε_0 and $\varepsilon_\perp$ are the vacuum and perpendicular dielectric constants, Γ_e^{na} and Γ_i^{na} are the neoclassical fluxes of electrons and ions, Γ_i^{lc} is the contribution from the loss cone loss of ions, Γ_i^{bv} is the flux driven by the bulk viscosity, Γ_i^{cx} is the contribution from the charge exchange ion loss and Γ_e^{beam} is the injected electron flux. For simplicity, the Reynolds stress and gyroviscosity [24] are neglected in Eq. (23). When the temperatures of electrons and ions are equal, electrons are more collisional than ions and the electron viscosity is a factor of about $(M_e/M_i)^{1/2}$ smaller than the ion viscosity. Therefore, the contributions of the loss

$$\Gamma_i^{nc} - \Gamma_e^{nc} + \Gamma_i^{lc} + \Gamma_e^{beam} = -\Gamma_i^{bv} - \Gamma_i^{cx}. \quad (24)$$

cone loss and the bulk viscosity of electrons are small compared to those of ions and therefore are neglected. The anomalous transport is assumed to be ambipolar In steady state, Eq. (23) is written as Equation (24) represents the momentum balance between the torque driven by the radial current (the left hand of Eq. (24)) and the damping force by the viscosity and ion-neutral interaction (the right hand of Eq. (24)).

With respect to the damping force induced flux,

$$\Gamma_i^{bv} = -2N\nu_d\left\{\frac{\sqrt{\pi}}{4}\sum_{m,n}\varepsilon_{mn}^2 m(m-nq) \times\left[I_{mn}\left(\frac{U_{//}}{v_t}+\frac{m}{m-nq}M_p-\frac{m}{m-nq}V_{p,P}\right) - L_{mn}\frac{m}{m-nq}V_{p,T}\right]\right\}, \quad (25)$$

$$\Gamma_i^{cx} = -2N\nu_d\varepsilon_t^2\frac{\nu_{eff}}{\nu_t/Rq} \times\left[\frac{U_{//}}{v_t}+\frac{1+2q^2}{q^2}\left(M_p-V_{p,P}\right)\right], \quad (26)$$

Γ_i^{bv} and Γ_i^{cx} are calculated as [22]
where $\nu_d = T/eBr$, $M_p = -E_r/B_p v_t$, $V_{p,p} = -p'/eN B_p v_t$, $V_{p,T} = -T/eB_p v_t$, p=dp/dr, T=dT/dr, N is the plasma density, T is the ion temperature, B_p is the poloidal magnetic field, v_t is the thermal velocity, q is the safety factor, ε_t is the toroidal ripple, m and n are the poloidal and toroidal mode numbers, with ε_{mn} corresponding helical ripples, I_{mn}, L_{mn} and ν_{eff} are defined in Ref. [21] and $U_{//}$ is the parallel flow velocity. The Fourier spectra of B in Hamada coordinates are used in these equations. In tokamaks, an explanation of the mechanism of the bifurcation of the radial electric field is based on the

existence of a local maximum in the bulk ion viscosity as a function of M_p [20]. In LHD configurations, the dependence of the poloidal viscosity on radial electric field is not similar to that for an axisymmetric configuration. The poloidal viscosity in LHD consists of more than two components [25], one being the toroidal component, contributed from the toroidal ripple, and the other being the helical component, contributed from the helical ripples. Each of the components has a local maximum. The local maxima induced by the helical components (helical maxima) are located in a region of larger M_p than the toroidal maximum, and hence the toroidal maximum is overshadowed by the helical maxima. Thus, the first local maxima in the bulk ion viscosity for LHD configurations exist in a larger M_p region compared with axisymmetric configurations This may be unfavorable from the point of view of the realization of bifurcation. In an outer shifted LHD configuration (R_{ax} = 3.9 m), the first local maximum is located in a smaller M_p region compared to an inner shifted configuration [25], and hence the possibility of bifurcation of M_p is discussed in the outer shifted configuration in this section. In the outer shifted configuration, however, the particle orbit properties deteriorate and the bulk heating efficiency of the neutral beam may become worse compared to the inner shifted configuration [26]. These effects are not taken into account here.

$$\Gamma_i^{lc} = 2N\nu_d\varepsilon_t^{3/2}\frac{\nu_*}{\sqrt{\nu_* + (0.5M_p)^4}} \times \exp\left[-\sqrt{\nu_* + (0.5M_p)^4}\right], \quad (27)$$

In the edge region (about one poloidal ion gyroradius, ρ_p, away from the boundary) of LHD, the ion orbit can intersect the last closed magnetic surface. The ion orbit loss associated with the tokamak-like banana orbit is estimated as [20] where $\nu_* = (\nu_i/\varepsilon_t)/[\varepsilon_t^{1/2}(\nu_i/Rq)]$. Because electrons are more collisional than ions, the orbit loss of electrons is neglected. The helically trapped particles may also contribute Γ_i^{lc}. The collisionality of collisionless helically trapped particle, expressed as $\nu_{*h}^{h} = (\nu_i/\varepsilon_h)/[(\nu_i/Rq)|\varepsilon_h\rho_p/r - M_p|]$, is larger than that of toroidally trapped particles, ν_*, if $\varepsilon_t \sim \varepsilon_h$ and $M_p \gg \varepsilon_h\rho_p/r$, where ε_h is the dominant component of the helical ripples. And furthermore, the loss cone loss of the helically trapped particles is important in the region about $\varepsilon_t\rho_p/M_p$ away from the boundary. We are interested in the large M_p region ($M_p \geq 1$), the direct loss associated with the drift orbit of helically trapped particles is thus not important

$$\Gamma_i^{nc} = -2N\nu_d\frac{\varepsilon_t^2}{|m-nq|\nu_*^h} \times\left[I_{1i}(M_p - V_{p,p}) - I_{2i}V_{p,T}\right], \quad (28)$$

compared to the tokamak-like banana orbit loss and therefore, not taken into account. The low collisionality helically trapped particles, however, drive the transport flux and contribute the radial current. This non-axisymmetric effect is taken into account and the neoclassical flux are given as [21] where $\nu_*^h = (\nu_i/\varepsilon_t)/[\varepsilon_h^{1/2}(\nu_i|m-nq|/Rq)]$, I_{1i} and I_{2i} are defined in Ref. [20]. The electron flux, which is similar to Eq. (28), is also given in Ref. [20]. In these equations, the different collisional regimes are connected smoothly with respect to the collisionality. As concerns Γ_e^{beam}, the beam energy, the pitch angle and launching point are chosen so that the electron can penetrate the core region and we assume that all the electrons, which are injected using the loss cone, are detrapped in the core region. If electrons are deposited in the plasma, the radial electric field will be changed. The change of the radial electric field influences the detrapping points of the injected electrons. The beam flux passing through the edge region, however, will be little affected by the change of the detrapping point. The injected electron beam flux, Γ_e^{beam}, is thus assumed to not depend on M_p as far as edge region.

3.2. Bifurcation Feature on LHD

The equilibrium of M_p is determined by plotting the left and right sides of Eq. (24) as a function M_p. For the configuration parameter, ε_t = 0.16, ε_h = 0.095, m=4, n=10, q=0.8, B_0 = 3T are used and $U_{//}/\nu_i$ =0, Γ_e^{beam} =6×10^{18} $m^{-2}s^{-1}$ are assumed. In Fig. 10, the edge temperature is low and M_p is small (see an intersection of the solid curve and the broken curve). In this case, a drastic change in M_p is not expected if the electron beam is injected (see an intersection of two solid curves). When the temperature increases and ν_* decreases, M_p can have three solutions if the electron beam is injected, as shown in Fig. 11. In this situation, there is a strong possibility to introduce the bifurcation of M_p. If the bifurcation occurs and M_p becomes large enough, the ion energy confinement may be improved. In the case that the confinement is improved and the edge temperature becomes high enough, only a large M_p solution exists, as shown in Fig. 12. Furthermore, M_p remains large, even if the electron beam is turned-off. This feature suggests

that the electron beam injection can be used just as a trigger for introducing the bifurcation of M_p

The qualitative results of a similar model described here are in good agreement with the experimental measurements in tokamaks and in a helical system [20, 22]. Hence the existence of the local maximum in viscosity will explain the qualitative behavior of M_p on LHD and therefore the bifurcation of M_p is expected by means of the electron beam injection

It is expected that a large M_p in the core region will be produced if the electron beam can penetrate to the core region. The behavior of M_p in the core region will be similar to that in the edge region except that the ion orbit loss associated with the tokamak-like banana orbit is not present. In this case, the ion orbit loss associated with drift orbit of helically trapped particles will become important. Like the electron beam injection, the ion beam injection will be used as a means of controlling E_r. If the high energy ions are injected by using the loss cone or drift island motion [27], a negative M_p (positive E_r) is expected.

From the point of view of confinement improvement, it is necessary that the energy for driving a large E_r is less than the increase in the bulk energy resulting from the development of E_r. Therefore, it will be important to evaluate the power balance. It seems that the outer shifted configuration is favorable to the electron beam injection. In the outer shifted configuration case, however, the orbit loss, namely, the energy loss may be enhanced. And hence, the bulk temperature may not be high enough to become a good target for the electron beam injection. The calculation of the orbit loss, which is self-consistent with the E_r profile as well as the related evaluation of the power partition will be carried out in the future.

One can conclude that the electron beam injection has a strong possibility of driving M_p to a large extent. And we emphasize that the electron beam is used as the trigger for introducing the bifurcation of M_p and confinement improvement.

4. Summary

As the result of our study to control the electric field in plasmas of a helical device with the use of the electron beam, it is possible to conclude the following.

1. The penetration of high energy electrons or ions to the core of the plasma in a helical device is demonstrated by the drift orbit calculation, this is the case of the electrons belonging to the "loss cone", namely, the case in which trajectories are the "transit orbits". It is possible to launch helically trapped particles from the outside of the magnetic confinement volume and then transform them into blocked particles in the center of the confinement volume

2. High energy electrons can stay in the core of the plasma long enough before retrapping occurs. It is sufficient to form a non-ambipolar flux across the magnetic surfaces and which functions to form the radial electric field.

3. The life time of the injected electrons staying as blocked particles in the core can be made long enough if an AC electric field, parallel to the magnetic force line, is applied.

4. Due to the help of an AC electric field, not only particles with the transit orbits can penetrate to the core of the plasma. Even the helically trapped particles with smaller $V_{//}/V$, the so called deeply helically trapped ones, are also possibly utilized if the AC electric field can transform the deeply helically trapped particles into blocked particles.

5. The electron beam injection has a strong possibility to triger the bifurcation of M_p in the edge region of the LHD plasma.

Acknowledgments

One of the authors (A.A.Shishkin) would like to express his deep gratitude to Prof. K. Yamazaki, Prof. M. Fujiwara and Director General Prof. A. Iiyoshi for the possibility to come to NIFS and take part in this investigation. Authors are grateful too to Dr. Peterson for his help in brushing up our paper to a great extent.

References

[1] IIYOSHI, A., FUJIWARA, M., MOTOJIMA, O., OHYABU, N., YAMAZAKI, K., Fusion Technology 17 (1997) 169.

[2] MOTOJIMA, O , Fusion Engineering and Design 39-40 (1998) 91.

[3] GALEEV, A. A., SAGDEEV, R. Z., Reviews of Plasma Physics (Edit. by Acad. M. A. Leontopvich) vol.7, 1979, Consultants Bureau New York-London, p. 257-343.

[4] CHOE,W.,ONO, M., CHANG, C.-S., Nuclear Fusion **36** (1996) 1703.
[5] ITOH, K., SANUKI, H., TODOROKI, T., ITOH, S.-I., FUKUYAMA, A., HANATANI., K., Phys.Fluids B **3** (1991) 1294
[6] GIBSON, A., Taylor, J.B., Phys.Fluids **10** (1967) 2653.
[7] DOBROTT, D., FRIEMAN, E.A., Phys.Fluids **14** (1971) 349.
[8] DOBROTT, D., GREENE, J.M., Phys.Fluids **14** (1971) 1525.
[9] WAKATANI, M., KODAMA, S , NAKASUGA, M., HANATANI, K. Nuclear Fusion **21** (1981) 175.
[10] MYNICK, H.E., Phys.Fluids **26** (1983) 1008.
[11] MYNICK, H.E., Phys.Fluids **26** (1983) 2609.
[12] SANUKI, H., TODOROKI, J., KAMIMURA, T., Phys.Fluids **B2** (1990) 2155
[13] SHISHKIN, A.A., WATANABE, K.Y., YAMAZAKI, K., MOTOJIMA, O., GREKOV, D.L., SMIRNOVA, M.S. AND ZOLOTUKHIN, A.V. "Some Features of Particle Orbit Behavior in LHD Configurations", Research Report NIFS-211, March 1993, Nagoya, Japan.
[14] MOROZOV, A.I., SOLOV'EV, L.S. "Motion of Charged Particles in Electromagnetic Fields", in Reviews of Plasma Physics, Edited by Acad. M.A, Leontovich, vol.2, Consultants Bureau, New York, 1966, p. 201-297.
[15] DOBROWOLNY, M., POGUTSE, O.P., Phys.Rev.Letters **25** (1970) No.23, p.1608.
[16] DEMIRKHANOV, R.A., STOTLAND, M.A., KHIL', SH.V., Soviet Physics-Technical Physics **17** (1973) No.7, 1973, p.1128.
[17] VOITSENYA, V.S., VOLOSHKO, A. YU., KALINICHENKO, S.S., SOLODOVCHENKO, S.I., SHTAN', A.F., Sov. J. Plasma Physics **3** (6), Nov.-Dec. 1977, p.659.
[18] Biglari, H., Diamond, P. H., Terry, P. W., Phys. Fluids B2 (1990) 1.
[19] Shaing, K. C., Crume, Jr. E. C,. Houlberg, W. A., Phys. Fluids B2 (1990) 1492.
[20] Shaing, K. C.,. Crume, Jr. E. C., Phys. Rev. Lett. **63** (1989) 2369.
[21] Shaing, K. C., Phys. Fluids **27** (1984) 1567.
[22] Shaing, K. C., Phys. Rev. Lett. **76** (1996) 4364.
[23] Itoh K., Itoh S-I., Plasma Phys. Control. Fusion **38** (1996) 1.
[24] Connor, J. W, S. Cowley, S. C., Hastie, R. J., Pan, L. R., Plasma Phys. Control. Fusion **29** (1987) 931.
[25] Yokoyama, M., Nakajima, N., Okamoto M. "Nonlinear Incompressible Poloidal Viscosity in L=2 Heliotron and Quasi-Symmetric Stellarators", Research Report NIFS-519, Nov. 1997, Nagoya, Japan.
[26] Sanuki, H, Itoh K., Itoh S-I., J. Phys. Soc. Jpn. **62** (1993) 123.
[27] Motojima, O., Shishkin, A. A., Plasma Phys. Control. Fusion **41** (1999) 227.

Figure Captions

Fig. 1. Transition curves under the values of $V_{//0}/V$ = 0.01, 0.11, 0.21, 0.31 and $e\phi_0/\mu B_0$ = 0.0 (a) and $V_{//0}/V$ = 0.31, $e\phi_0/\mu B_0$ = - 0.4, 0.0, 0.4 (b)

Fig. 2. Electric field profile in two directions ϑ=0 (a) and ϑ=π/4 (b).

Fig. 3. Projections of the trajectory of a transit particle on the vertical (a) and horizontal (b) planes .

Fig. 4 3D trajectory of a transit particle (a) and the change of $V_{//}/V$ in time (b).

Fig. 5. 3D trajectory (a) and the change of $V_{//}/V$ in time (b) of a transit particle with AC electric field.

Fig. 6. The change of $V_{//}/V$ in time without AC electric field (1) and with AC electric field (2) at the moment of detrapping (a) and retrapping (b) for the case $\widetilde{E}_\varphi / E = 0$; here the dependence of the AC electric field on time (3) is shown also.

Fig. 7. 3D trajectories of the helically trapped particles without AC electric field (a), with AC electric field under $\widetilde{E}_\varphi / E = 0.15$, Ω= (3/2)ω_b (b) and under $\widetilde{E}_\varphi / E = 0.2$, Ω=(5/2)ω_b (c).

Fig. 8. The change of $V_{//}/V$ in time for the particles in Fig.7.

Fig. 9. The staying time of a particle in the core of plasma, τ, dependence on the radial position of the launching point, r_0, for the configuration with an inward shift of the magnetic axis.

Fig. .10 The left side and the right side of Eq.(24) versus M_p for low temperature and ν^* = 16. The left side without the electron beam is also shown (dashed line).

Fig. 11 The left side and the right side of Eq (24) versus M_p for moderate temperature and $\nu^* = 12$ The M_p can have three solutions if the electron beam is injected. The middle root is unstable.

Fig .12 The left side and the right side of Eq.(24) versus M_p for high temperature and $\nu^* = 5.9$ There is only one, large solution for M_p even if the electron beam is turned off.

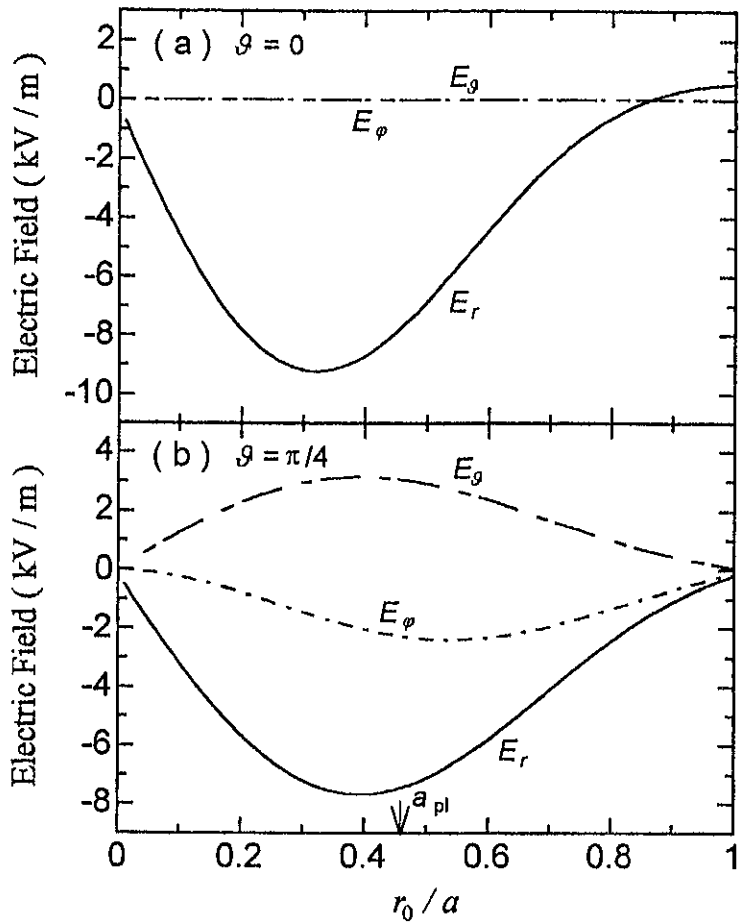
(a) $\vartheta = 0$
E_ϑ
E_φ
E_r
(b) $\vartheta = \pi/4$
E_ϑ
E_φ
E_r
a_{pl}
Electric Field (kV / m)
Electric Field (kV / m)
r_0 / a

Fig. 2

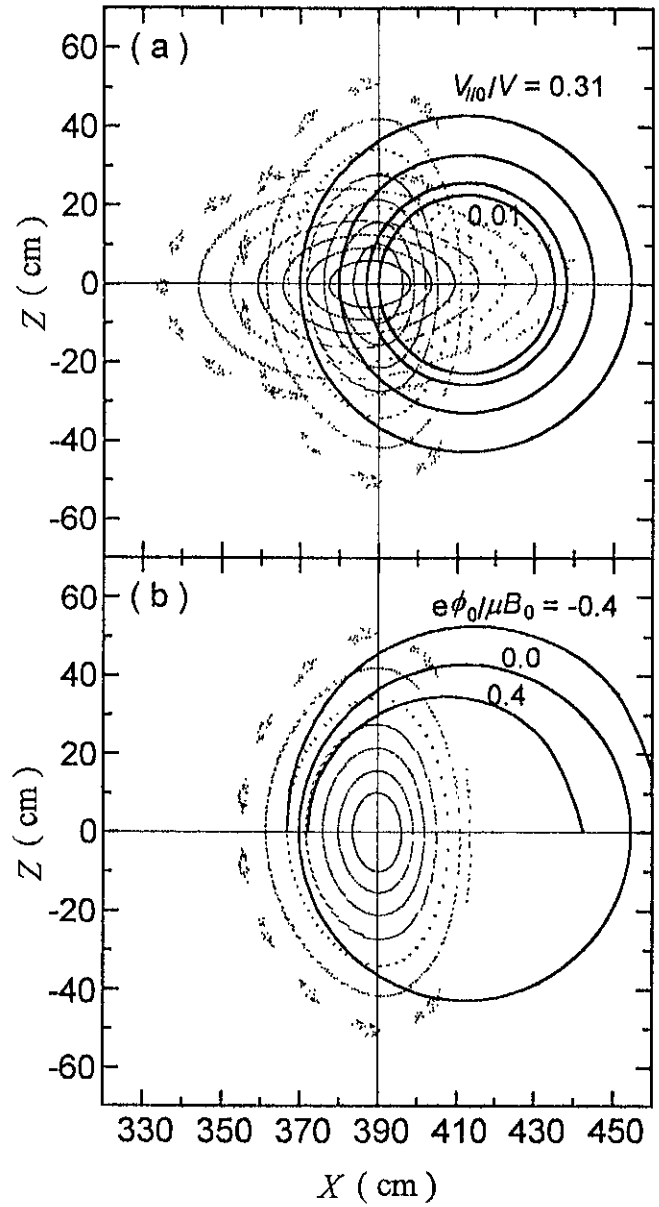
(a)
$V_{//0}/V = 0.31$
0.01
(b)
$e\phi_0/\mu B_0 = -0.4$
0.0
0.4
Z (cm)
Z (cm)
X (cm)

Fig. 1

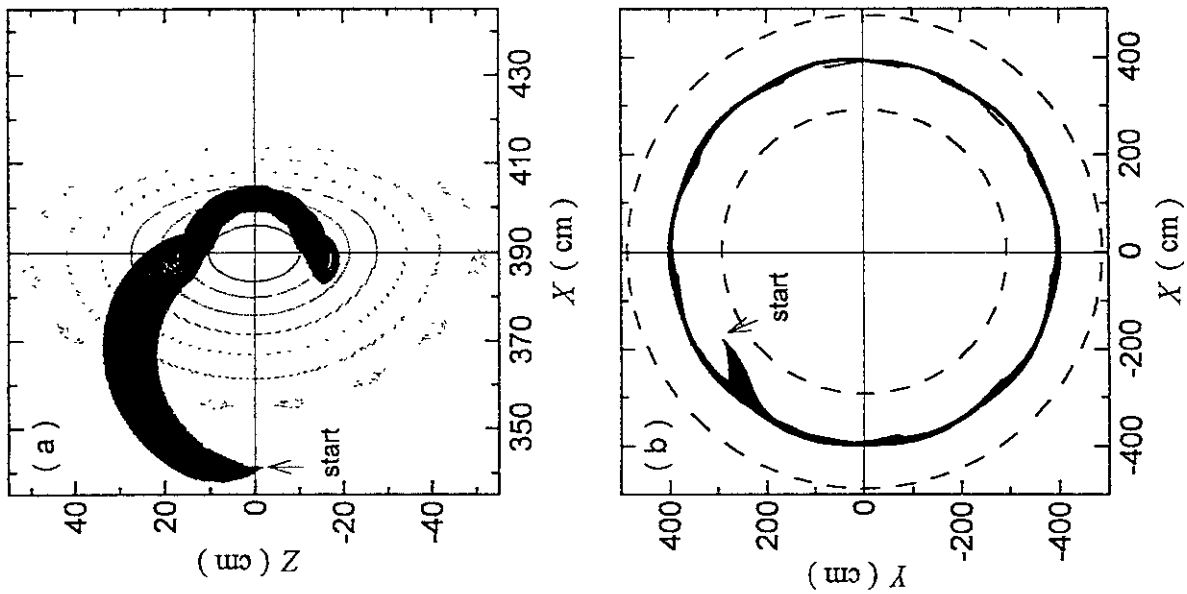
(a)
start
Z (cm)
X (cm)
(b)
start
Y (cm)
X (cm)

Fig. 3

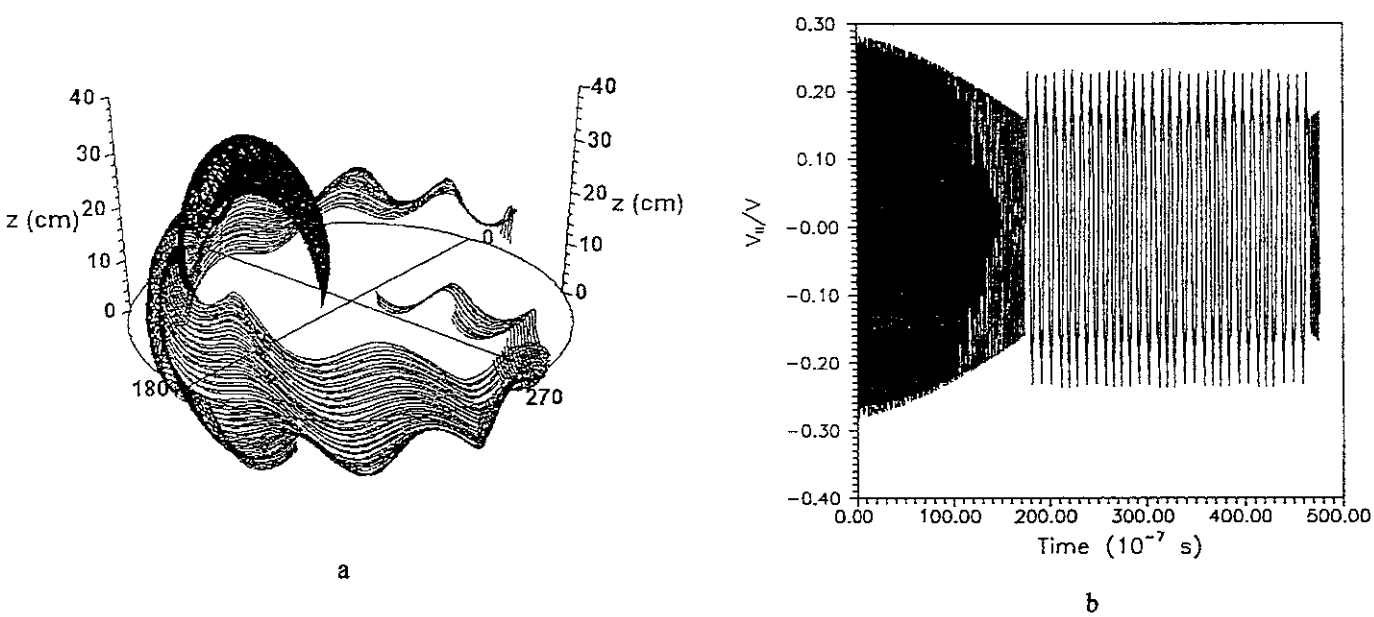
z (cm)
z (cm)
180
270
$V_{\parallel}/V$
Time (10^{-7} s)

a b

Fig. 4

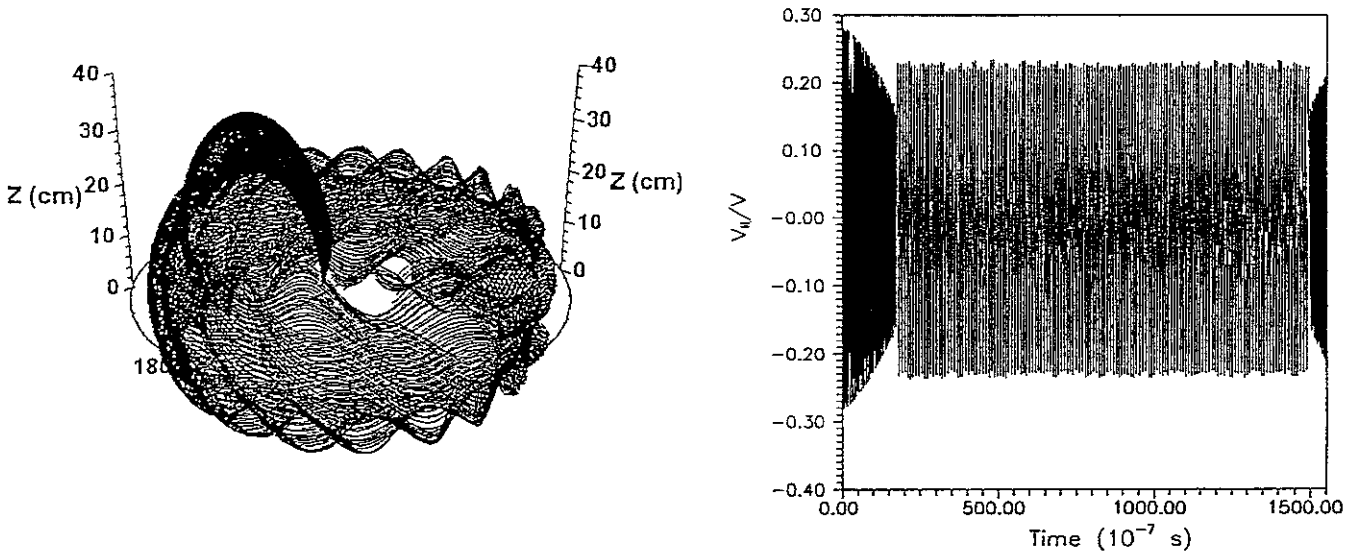
Z (cm)
40
30
20
10
0
180
Z (cm)
$V_{\parallel}/V$
0.30
0.20
0.10
−0.00
−0.10
−0.20
−0.30
−0.40
0.00
500.00
1000.00
1500.00
Time (10^{-7} s)

a

b

Fig. 5

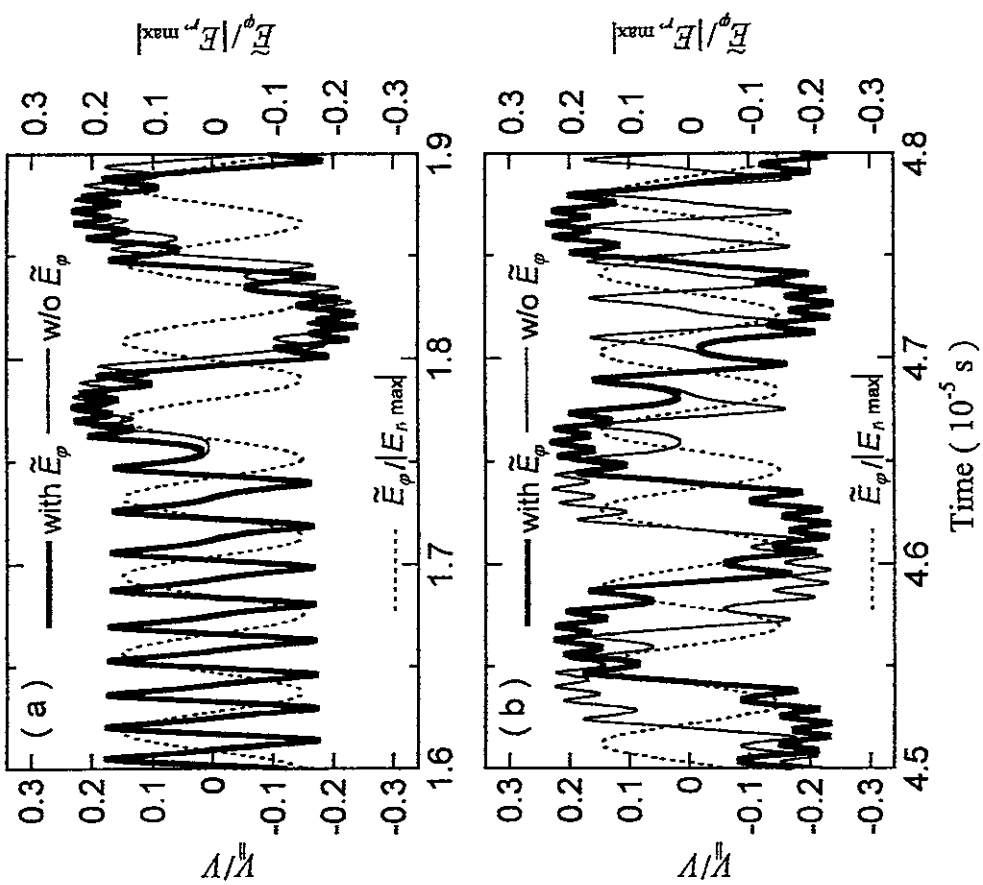
$\tilde{E}_\phi/|E_{r,\max}|$
$V_{\parallel}/V$
with $\tilde{E}_\phi$
w/o $\tilde{E}_\phi$
$\tilde{E}_\phi/|E_{r,\max}|$
(a)
(b)
Time (10^{-5} s)

Fig. 6

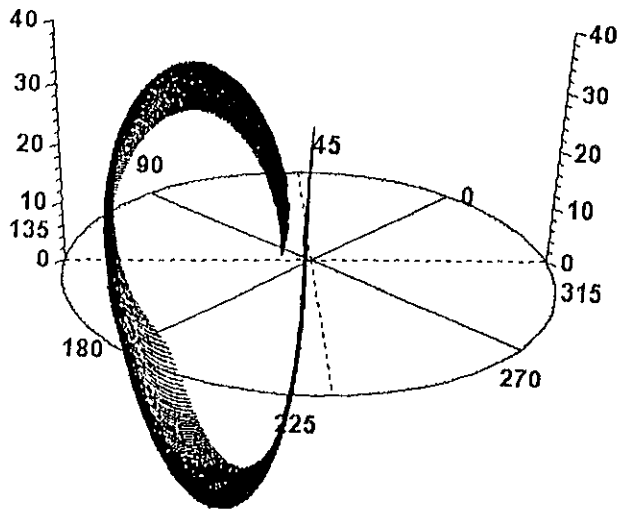
40
30
20
10
135
0
90
45
0
180
270
225
40
30
20
10
0
315

a

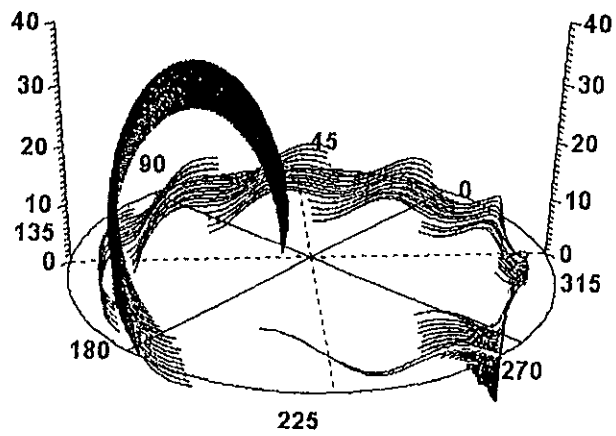
40
30
20
10
135
0
90
45
0
180
270
225
40
30
20
10
0
315

b

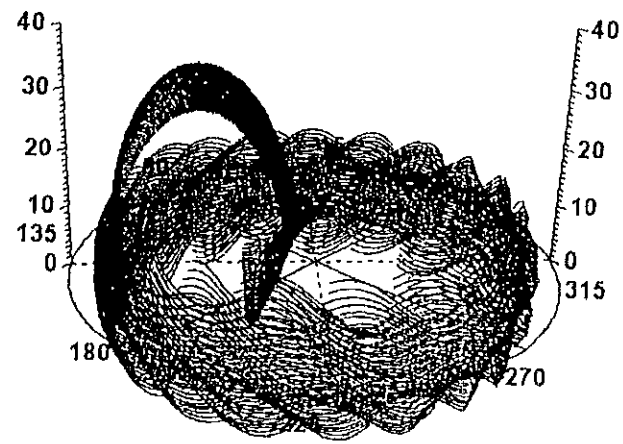
40
30
20
10
135
0
180
270
40
30
20
10
0
315

c

Fig. 7

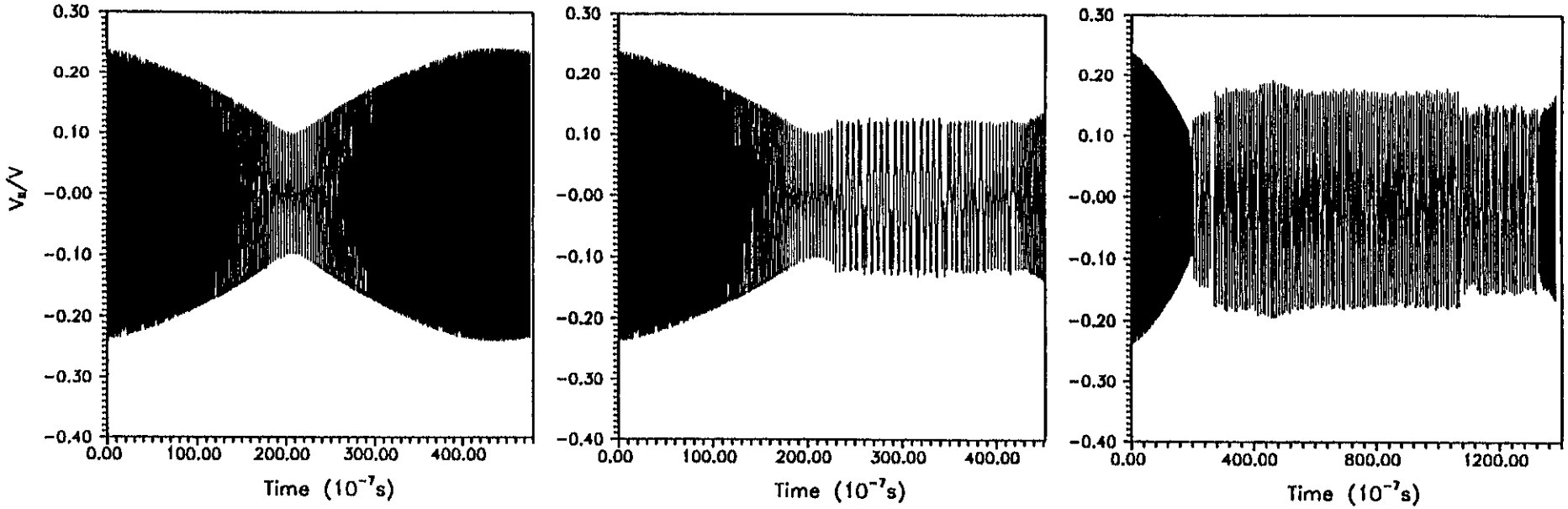
0.30
0.20
0.10
-0.00
-0.10
-0.20
-0.30
-0.40
V_R/V
0.00
100.00
200.00
300.00
400.00
Time (10^{-7}s)
a
0.00
100.00
200.00
300.00
400.00
Time (10^{-7}s)
b
0.00
400.00
800.00
1200.00
Time (10^{-7}s)
c

Fig. 8

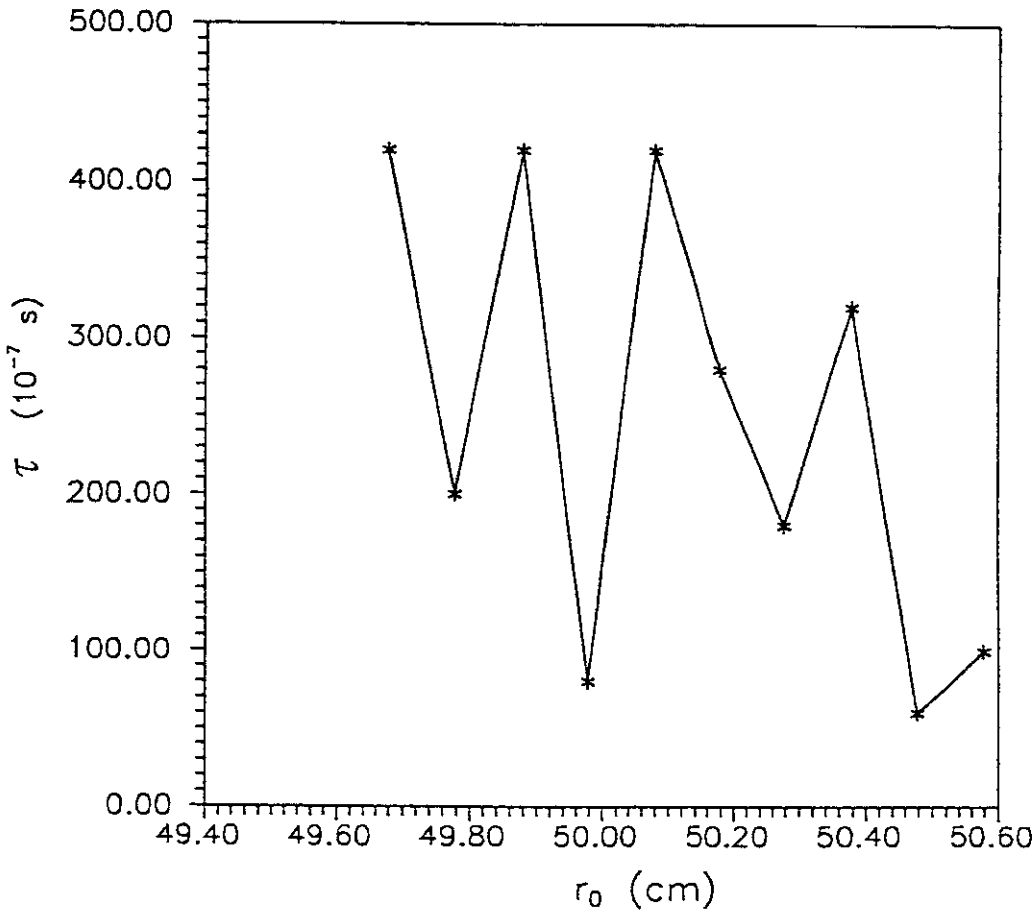
500.00
400.00
300.00
200.00
100.00
0.00
τ (10⁻⁷ s)
49.40
49.60
49.80
50.00
50.20
50.40
50.60
r₀ (cm)

Fig. 9

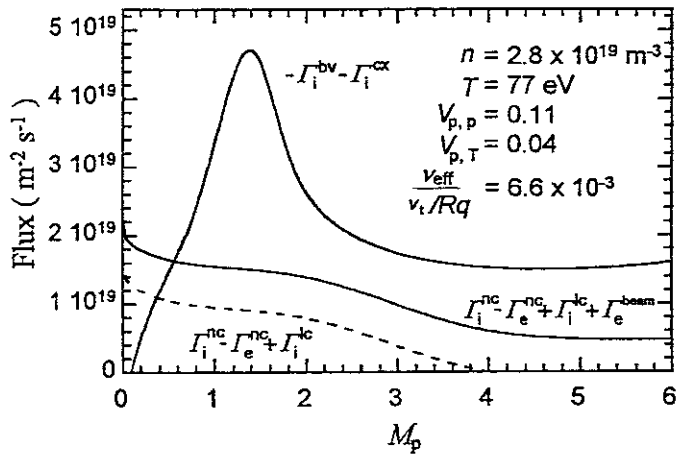

Fig. 10

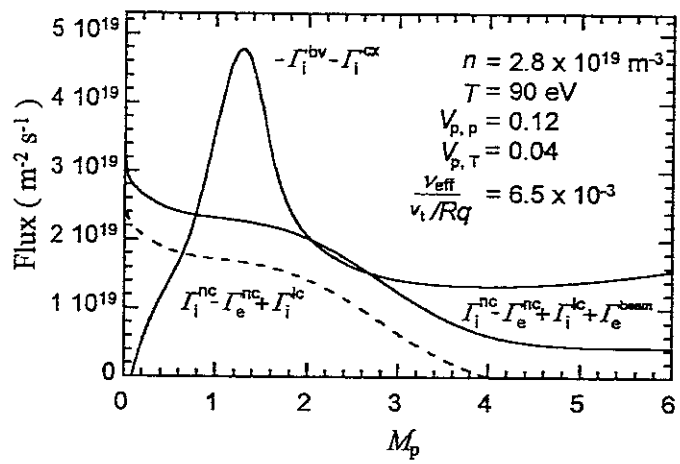

Fig. 11

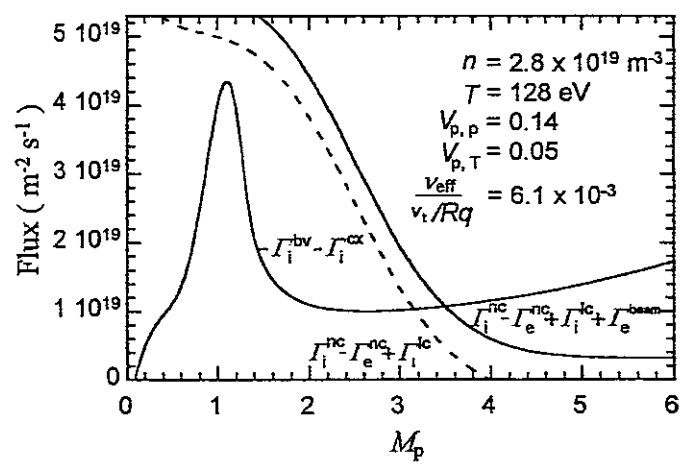

Fig. 12

Recent Issues of NIFS Series

NIFS-544 J Uramoto,
Simplified ν_μ bar{ν}$_\mu$ Beam Detector and ν_μ bar{ν}$_\mu$ Beam Source by Interaction between an Electron Bunch and a Positive Ion Bunch; Mar. 1998

NIFS-545 J. Uramoto,
Various Neutrino Beams Generated by D_2 Gas Discharge, Mar 1998

NIFS-546 R. Kanno, N Nakajima, T. Hayashi and M Okamoto,
Computational Study of Three Dimensional Equilibria with the Bootstrap Current; Mar. 1998

NIFS-547 R. Kanno, N. Nakajima and M. Okamoto,
Electron Heat Transport in a Self-Similar Structure of Magnetic Islands; Apr. 1998

NIFS-548 J.E. Rice,
Simulated Impurity Transport in LHD from MIST; May 1998

NIFS-549 M.M. Skoric, T. Sato, A.M Maluckov and M.S Jovanovic,
On Kinetic Complexity in a Three-Wave Interaction; June 1998

NIFS-550 S. Goto and S Kida,
Passive Saclar Spectrum in Isotropic Turbulence: Prediction by the Lagrangian Direct-interaction Approximation; June 1998

NIFS-551 T Kuroda, H. Sugama, R Kanno, M. Okamoto and W Horton,
Initial Value Problem of the Toroidal Ion Temperature Gradient Mode ; June 1998

NIFS-552 T. Mutoh, R. Kumazawa, T. Seki, F. Simpo, G. Nomura, T. Ido and T. Watari,
Steady State Tests of High Voltage Ceramic Feedthoughs and Co-Axial Transmission Line of ICRF Heating System for the Large Helical Device ; June 1998

NIFS-553 N. Noda, K Tsuzuki, A Sagara, N. Inoue, T. Muroga,
oronaization in Future Devices -Protecting Layer against Tritium and Energetic Neutrals-: July 1998

NIFS-554 S. Murakami and H. Saleem,
Electromagnetic Effects on Rippling Instability and Tokamak Edge Fluctuations; July 1998

NIFS-555 H. Nakamura , K. Ikeda and S. Yamaguchi,
Physical Model of Nernst Element, Aug. 1998

NIFS-556 H. Okumura, S. Yamaguchi, H. Nakamura, K. Ikeda and K. Sawada,
Numerical Computation of Thermoelectric and Thermomagnetic Effects; Aug 1998

NIFS-557 Y Takeiri, M Osakabe, K Tsumori, Y Oka, O Kaneko, E Asano, T Kawamoto, R Akiyama and M. Tanaka,
Development of a High-Current Hydrogen-Negative Ion Source for LHD-NBI System; Aug 1998

NIFS-558 M. Tanaka, A Yu Grosberg and T. Tanaka,
Molecular Dynamics of Structure Organization of Polyampholytes; Sep 1998

NIFS-559 R. Horiuchi, K Nishimura and T. Watanabe,
Kinetic Stabilization of Tilt Disruption in Field-Reversed Configurations, Sep. 1998
(IAEA-CN-69/THP1/11)

NIFS-560 S Sudo, K. Kholopenkov, K Matsuoka, S. Okamura, C. Takahashi, R. Akiyama, A. Fujisawa, K. Ida, H Idei, H Iguchi, M. Isobe, S. Kado, K. Kondo, S. Kubo, H. Kuramoto, T. Minami, S Morita, S Nishimura, M. Osakabe, M. Sasao, B. Peterson, K. Tanaka, K. Toi and Y. Yoshimura,
Particle Transport Study with Tracer-Encapsulated Solid Pellet Injection; Oct 1998
(IAEA-CN-69/EXP1/18)

NIFS-561 A Fujisawa, H. Iguchi, S. Lee, K. Tanaka, T. Minami, Y. Yoshimura, M. Osakabe, K. Matsuoka, S. Okamura, H Idei, S. Kubo, S. Ohdachi, S. Morita, R. Akiyama, K Toi, H. Sanuki, K. Itoh, K. Ida, A Shimizu, S. Takagi, C Takahashi, M. Kojima, S. Hidekuma, S Nishimura, M Isobe, A. Ejiri, N. Inoue, R Sakamoto, Y. Hamada and M. Fujiwara,
Dynamic Behavior Associated with Electric Field Transitions in CHS Heliotron/Torsatron; Oct 1998

(IAEA-CN-69/EX5/1)

NIFS-562 S. Yoshikawa,
Next Generation Toroidal Devices; Oct. 1998

NIFS-563 Y. Todo and T. Sato,
Kinetic-Magnetohydrodynamic Simulation Study of Fast Ions and Toroidal Alfvén Eigenmodes; Oct. 1998
(IAEA-CN-69/THP2/22)

NIFS-564 T. Watari, T. Shimozuma, Y. Takeiri, R. Kumazawa, T. Mutoh, M. Sato, O. Kaneko, K. Ohkubo, S. Kubo, H. Idei, Y. Oka, M. Osakabe, T. Seki, K. Tsumori, Y. Yoshimura, R. Akiyama, T. Kawamoto, S. Kobayashi, F. Shimpo, Y. Takita, E. Asano, S. Itoh, G. Nomura, T. Ido, M. Hamabe, M. Fujiwara, A. Iiyoshi, S. Morimoto, T. Bigelow and Y.P. Zhao,
Steady State Heating Technology Development for LHD; Oct. 1998
(IAEA-CN-69/FTP/21)

NIFS-565 A. Sagara, K Y Watanabe, K. Yamazaki, O. Motojima, M. Fujiwara, O. Mitarai, S Imagawa, H. Yamanishi, H. Chikaraishi, A Kohyama, H. Matsui, T. Muroga, T. Noda, N. Ohyabu, T. Satow, A.A. Shishkin, S. Tanaka, T Terai and T. Uda,
LHD-Type Compact Helical Reactors; Oct. 1998
(IAEA-CN-69/FTP/03(R)

NIFS-566 N. Nakajima, J. Chen, K. Ichiguchi and M. Okamoto,
Global Mode Analysis of Ideal MHD Modes in L=2 Heliotron/Torsatron Systems; Oct. 1998
(IAEA-CN-69/THP1/08)

NIFS-567 K. Ida, M. Osakabe, K. Tanaka, T. Minami, S. Nishimura, S Okamura, A. Fujisawa, Y. Yoshimura, S. Kubo, R. Akiyama, D.S.Darrow, H. Idei, H. Iguchi, M. Isobe, S. Kado, T. Kondo, S. Lee, K. Matsuoka, S. Morita, I. Nomura, S. Ohdachi, M. Sasao, A. Shimizu, K. Tumori, S. Takayama, M Takechi, S. Takagi, C. Takahashi, K. Toi and T. Watari,
Transition from L Mode to High Ion Temperature Mode in CHS Heliotron/Torsatron Plasmas; Oct. 1998
(IAEA-CN-69/EX2/2)

NIFS-568 S. Okamura, K. Matsuoka, R. Akiyama, D.S. Darrow, A. Ejiri, A. Fujisawa, M. Fujiwara, M. Goto, K. Ida H. Idei, H. Iguchi, N. Inoue, M. Isobe, K. Itoh, S. Kado, K. Khlopenkov, T. Kondo, S. Kubo, A. Lazaros, S. Lee, G. Matsunaga, T. Minami, S. Morita, S. Murakami, N. Nakajima, N. Nikai, S. Nishimura, I. Nomura, S. Ohdachi, K. Ohkuni, M. Osakabe, R. Pavlichenko, B. Peterson, R. Sakamoto, H. Sanuki, M. Sasao, A. Shimizu, Y. Shirai, S. Sudo, S. Takagi, C. Takahashi, S. Takayama, M. Takechi, K. Tanaka, K. Toi, K. Yamazaki, Y. Yoshimura and T. Watari,
Confinement Physics Study in a Small Low-Aspect-Ratio Helical Device CHS; Oct 1998
(IAEA-CN-69/OV4/5)

NIFS-569 M.M. Skoric, T. Sato, A. Maluckov, M.S. Jovanovic,
Micro- and Macro-scale Self-organization in a Dissipative Plasma; Oct. 1998

NIFS-570 T. Hayashi, N. Mizuguchi, T-H. Watanabe, T. Sato and the Complexity Simulation Group,
Nonlinear Simulations of Internal Reconnection Event in Spherical Tokamak; Oct. 1998
(IAEA-CN-69/TH3/3)

NIFS-571 A. Iiyoshi, A. Komori, A. Ejiri, M. Emoto, H. Funaba, M. Goto, K. Ida, H. Idei, S. Inagaki, S. Kado, O. Kaneko, K. Kawahata, S. Kubo, R. Kumazawa, S. Masuzaki, T. Minami, J. Miyazawa, T. Morisaki, S. Morita, S. Murakami, S. Muto, T. Muto, Y. Nagayama, Y. Nakamura, H. Nakanishi, K. Narihara, K. Nishimura, N. Noda, T. Kobuchi, S. Ohdachi, N. Ohyabu, Y. Oka, M. Osakabe, T. Ozaki, B.J. Peterson, A. Sagara, S. Sakakibara, R. Sakamoto, H. Sasao, M. Sasao, K. Sato, M. Sato, T. Seki, T. Shimozuma, M. Shoji, H. Suzuki, Y. Takeiri, K. Tanaka, K. Toi, T. Tokuzawa, K. Tsumori, I. Yamada, H. Yamada, S. Yamaguchi, M. Yokoyama, K.Y.Watanabe, T. Watari, R. Akiyama, H. Chikaraishi, K. Haba, S. Hamaguchi, S. Iima, S. Imagawa, N. Inoue, K. Iwamoto, S. Kitagawa, Y. Kubota, J. Kodaira, R. Maekawa, T. Mito. T. Nagasaka, A. Nishimura, Y. Takita, C. Takahashi, K. Takahata, K. Yamauchi, H Tamura, T. Tsuzuki, S. Yamada, N. Yanagi, H. Yonezu, Y. Hamada, K. Matsuoka, K. Murai, K. Ohkubo, I Ohtake, M. Okamoto, S. Sato, T. Satow, S. Sudo, S Tanahashi, K. Yamazaki, M Fujiwara and O. Motojima,
An Overview of the Large Helical Device Project; Oct. 1998
(IAEA-CN-69/OV1/4)

NIFS-572 M. Fujiwara, H. Yamada, A. Ejiri, M. Emoto, H. Funaba, M. Goto, K. Ida, H. Idei, S. Inagaki, S. Kado, O. Kaneko, K. Kawahata, A. Komori, S. Kubo, R. Kumazawa, S. Masuzaki, T. Minami, J. Miyazawa, T. Morisaki, S. Morita, S. Murakami, S. Muto, T. Muto, Y. Nagayama, Y. Nakamura, H. Nakanishi, K. Narihara, K. Nishimura, N. Noda, T. Kobuchi, S. Ohdachi, N. Ohyabu, Y. Oka, M. Osakabe, T. Ozaki, B. J. Peterson, A. Sagara, S. Sakakibara, R. Sakamoto, H. Sasao, M. Sasao, K. Sato, M. Sato, T. Seki, T. Shimozuma, M. Shoji, H. Sazuki, Y. Takeiri, K. Tanaka, K. Toi, T. Tokuzawa, K. Tsumori, I. Yamada, S. Yamaguchi, M. Yokoyama, K.Y. Watanabe, T. Watari, R. Akiyama, H. Chikaraishi, K. Haba, S. Hamaguchi, M. Iima, S. Imagawa, N. Inoue, K. Iwamoto, S. Kitagawa, Y. Kubota, J. Kodaira, R. Maekawa, T. Mito, T. Nagasaka, A. Nishimura, Y. Takita, C. Takahashi, K. Takahata, K. Yamauchi, H. Tamura, T. Tsuzuki, S. Yamada, N. Yanagi, H. Yonezu, Y. Hamada, K. Matsuoka, K. Murai, K. Ohkubo, I. Ohtake, M. Okamoto, S. Sato, T. Satow, S. Sudo, S. Tanahashi, K. Yamazaki, O. Motojima and A. Iiyoshi,
Plasma Confinement Studies in LHD; Oct. 1998
(IAEA-CN-69/EX2/3)

NIFS-573 O. Motojima, K. Akaishi, H. Chikaraishi, H. Funaba, S. Hamaguchi, S. Imagawa, S. Inagaki, N. Inoue, A. Iwamoto, S. Kitagawa, A. Komori, Y. Kubota, R. Maekawa, S. Masuzaki, T. Mito, J. Miyazawa, T. Morisaki, T. Muroga, T. Nagasaka, Y. Nakmura, A. Nishimura, K. Nishimura, N. Noda, N. Ohyabu, S. Sagara, S. Sakakibara, R. Sakamoto, S. Satoh, T. Satow, M. Shoji, H. Suzuki, K. Takahata, H. Tamura, K. Watanabe, H. Yamada, S. Yamada, S. Yamaguchi, K. Yamazaki, N. Yanagi, T. Baba, H. Hayashi, M. Iima, T. Inoue, S. Kato, T. Kato, T. Kondo, S. Moriuchi, H. Ogawa, I. Ohtake, K. Ooba, H. Sekiguchi, N. Suzuki, S. Takami,

Y Taniguchi, T Tsuzuki, N. Yamamoto, K Yasui, H. Yonezu, M Fujiwara and A. Iiyoshi,
Progress Summary of LHD Engineering Design and Construction; Oct 1998
(IAEA-CN-69/FT2/1)

NIFS-574 K Toi, M Takechi, S Takagi, G Matsunaga, M Isobe, T Kondo, M Sasao, D S Darrow, K. Ohkuni, S Ohdachi, R. Akiyama A. Fujisawa, M Gotoh, H Idei, K. Ida, H Iguchi, S. Kado, M Kojima, S Kubo, S Lee, K. Matsuoka, T. Minami, S. Morita, N. Nikai, S Nishimura, S. Okamura, M Osakabe, A. Shimizu, Y. Shirai, C Takahashi, K Tanaka, T Watari and Y. Yoshimura,
Global MHD Modes Excited by Energetic Ions in Heliotron/Torsatron Plasmas;Oct 1998
(IAEA-CN-69/EXP1/19)

NIFS-575 Y Hamada, A Nishizawa, Y. Kawasumi, A Fujisawa, M. Kojima, K. Narihara, K Ida, A. Ejiri, S. Ohdachi, K. Kawahata, K Toi, K Sato, T. Seki, H Iguchi, K. Adachi, S. Hidekuma, S.Hirokura, K. Iwasaki, T Ido, R Kumazawa, H. Kuramoto, T. Minami, I Nomura, M Sasao, K.N. Sato, T Tsuzuki, I Yamada and T. Watari,
Potential Turbulence in Tokamak Plasmas,Oct 1998
(IAEA-CN-69/EXP2/14)

NIFS-576 S Murakami, U. Gasparino, H Idei, S. Kubo, H Maassberg, N. Marushchenko, N Nakajima, M Romé and M. Okamoto,
5D Simulation Study of Suprathermal Electron Transport in Non-Axisymmetric Plasmas;Oct 1998
(IAEA-CN-69/THP1/01)

NIFS-577 S Fujiwara and T Sato,
Molecular Dynamics Simulation of Structure Formation of Short Chain Molecules; Nov 1998

NIFS-578 T. Yamagishi,
Eigenfunctions for Vlasov Equation in Multi-species Plasmas Nov. 1998

NIFS-579 M. Tanaka, A Yu Grosberg and T Tanaka,
Molecular Dynamics of Strongly-Coupled Multichain Coulomb Polymers in Pure and Salt Aqueous Solutions,Nov. 1998

NIFS-580 J Chen, N. Nakajima and M Okamoto,
Global Mode Analysis of Ideal MHD Modes in a Heliotron/Torsatron System: I. Mercier-unstable Equilibria;Dec 1998

NIFS-581 M. Tanaka, A Yu Grosberg and T Tanaka,
Comparison of Multichain Coulomb Polymers in Isolated and Periodic Systems: Molecular Dynamics Study; Jan 1999

NIFS-582 V.S Chan and S Murakami,
Self-Consistent Electric Field Effect on Electron Transport of ECH Plasmas, Feb 1999

NIFS-583 M Yokoyama, N Nakajima, M Okamoto, Y. Nakamura and M. Wakatani,
Roles of Bumpy Field on Collisionless Particle Confinement in Helical-Axis Heliotrons,Feb. 1999

NIFS-584 T -H. Watanabe, T. Hayashi, T Sato, M. Yamada and H Ji,
Modeling of Magnetic Island Formation in Magnetic Reconnection Experiment,Feb 1999

NIFS-585 R. Kumazawa, T Mutoh, T. Seki, F Shinpo, G Nomura, T. Ido, T. Watari, Jean-Marie Noterdaeme and Yangping Zhao,
Liquid Stub Tuner for Ion Cyclotron Heating,Mar. 1999

NIFS-586 A Sagara, M Iima, S. Inagaki, N Inoue, H Suzuki, K. Tsuzuki, S. Masuzaki, J. Miyazawa, S. Morita, Y Nakamura, N. Noda, B. Peterson, S Sakakibara, T. Shimozuma, H. Yamada, K. Akaishi, H Chikaraishi, H. Funaba, O. Kaneko, K. Kawahata, A. Komori, N Ohyabu, O Motojima, LHD Exp. Group 1, LHD Exp. Group 2,
Wall Conditioning at the Starting Phase of LHD;Mar 1999

NIFS-587 T Nakamura and T Yabe,
Cubic Interpolated Propagation Scheme for Solving the Hyper-Dimensional Vlasov-Poisson Equation in Phase Space;Mar 1999

NIFS-588 W.X Wnag, N. Nakajima, S. Murakami and M Okamoto,
An Accurate δf Method for Neoclassical Transport Calculation;Mar. 1999

NIFS-589 K. Kishida, K. Araki, S Kishiba and K. Suzuki,
Local or Nonlocal? Orthonormal Divergence-free Wavelet Analysis of Nonlinear Interactions in Turbulence;Mar 1999

NIFS-590 K. Araki, K. Suzuki, K. Kishida and S. Kishiba,
Multiresolution Approximation of the Vector Fields on T^3; Mar. 1999

NIFS-591 K. Yamazaki, H. Yamada, K.Y.Watanabe, K. Nishimura, S. Yamaguchi, H. Nakanishi, A. Komori, H. Suzuki, T. Mito, H. Chikaraishi, K. Murai, O. Motojima and the LHD Group,
Overview of the Large Helical Device (LHD) Control System and Its First Operation; Apr. 1999

NIFS-592 T. Takahashi and Y. Nakao,
Thermonuclear Reactivity of D-T Fusion Plasma with Spin-Polarized Fuel; Apr. 1999

NIFS-593 H. Sugama,
Damping of Toroidal Ion Temperature Gradient Modes; Apr. 1999

NIFS-594 Xiaodong Li ,
Analysis of Crowbar Action of High Voltage DC Power Supply in the LHD ICRF System; Apr. 1999

NIFS-595 K. Nishimura, R. Horiuchi and T. Sato,
Drift-kink Instability Induced by Beam Ions in Field-reversed Configurations; Apr. 1999

NIFS-596 Y. Suzuki, T-H. Watanabe, T. Sato and T. Hayashi,
Three-dimensional Simulation Study of Compact Toroid Plasmoid Injection into Magnetized Plasmas; Apr. 1999

NIFS-597 H. Sanuki, K. Itoh, M. Yokoyama, A. Fujisawa, K. Ida, S. Toda, S.-I. Itoh, M. Yagi and A. Fukuyama,
Possibility of Internal Transport Barrier Formation and Electric Field Bifurcation in LHD Plasma; May 1999

NIFS-598 S. Nakazawa, N Nakajima, M. Okamoto and N. Ohyabu,
One Dimensional Simulation on Stability of Detached Plasma in a Tokamak Divertor; June 1999

NIFS-599 S. Murakami, N. Nakajima, M. Okamoto and J. Nhrenberg,
Effect of Energetic Ion Loss on ICRF Heating Efficiency and Energy Confinement Time in Heliotrons; June 1999

NIFS-600 R. Horiuchi and T. Sato,
Three-Dimensional Particle Simulation of Plasma Instabilities and Collisionless Reconnection in a Current Sheet;; June 1999

NIFS-601 W. Wang, M. Okamoto, N. Nakajima and S. Murakami,
Collisional Transport in a Plasma with Steep Gradients; June 1999

NIFS-602 T. Mutoh, R. Kumazawa, T. Saki, K. Saito, F. Simpo, G. Nomura, T. Watari, X. Jikang, G. Cattanei, H. Okada, K. Ohkubo, M. Sato, S. Kubo, T. Shimozuma, H. Idei, Y. Yoshimura, O. Kaneko, Y. Takeiri, M. Osakabe, Y. Oka, K. Tsumori, A. Komori, H. Yamada, K. Watanabe, S. Sakakibara, M. Shoji, R. Sakamoto, S. Inagaki, J. Miyazawa, S. Morita, K. Tanaka, B.J. Peterson, S. Murakami, T. Minami, S. Ohdachi, S. Kado, K. Narihara, H. Sasao, H. Suzuki, K. Kawahata, N. Ohyabu, Y. Nakamura, H. Funaba, S. Masuzaki, S. Muto, K. Sato, T. Morisaki, S. Sudo, Y. Nagayama, T. Watanabe, M. Sasao, K.. Ida, N. Noda, K. Yamazaki, K. Akaishi, A. Sagara, K. Nishimura, T. Ozaki, K. Toi, O. Motojima, M. Fujiwara, A. Iiyoshi and LHD Exp. Group 1 and 2,
First ICRF Heating Experiment in the Large Helical Device; July 1999

NIFS-603 P.C. de Vries, Y Nagayama, K. Kawahata, S. Inagaki, H. Sasao and K. Nagasaki,
Polarization of Electron Cyclotron Emission Spectra in LHD; July 1999

NIFS-604 W. Wang, N. Nakajima, M. Okamoto and S. Murakami,
δf Simulation of Ion Neoclassical Transport; July 1999

NIFS-605 T. Hayashi, N. Mizuguchi, T. Sato and the Complexity Simulation Group,
Numerical Simulation of Internal Reconnection Event in Spherical Tokamak; July 1999

NIFS-606 M. Okamoto, N. Nakajima and W. Wang,
On the Two Weighting Scheme for δf Collisional Transport Simulation; Aug. 1999

NIFS-607 O. Motojima, A.A. Shishkin, S. Inagaki, K. Y. Watanabe,
Possible Control Scenario of Radial Electric Field by Loss-Cone-Particle Injection into Helical Device; Aug. 1999